Published in final edited form as:
Cell. 2011 October 28; 147(3): 603–614. doi:10.1016/j.cell.2011.08.048.

Altered Modes of Stem Cell Division Drive Adaptive Intestinal Growth

Lucy Erin O'Brien, **Sarah S. Soliman**, **Xinghua Li**, and **David Bilder**
Department of Molecular and Cell Biology, University of California, Berkeley, California 94720 USA

Summary

Throughout life, adult organs continually adapt to variable environmental factors. Adaptive mechanisms must fundamentally differ from homeostatic maintenance, but little is known about how physiological factors elicit tissue remodeling. Here, we show that specialized stem cell responses underlie the adaptive resizing of a mature organ. In the adult Drosophila midgut, intestinal stem cells interpret a nutrient cue to 'break homeostasis' and drive growth when food is abundant. Activated in part by niche production of insulin, stem cells direct a growth program through two altered modes of behavior: accelerated division rates and predominance of symmetric division fates. Together, these altered modes produce a net increase in total intestinal cells, which is reversed upon withdrawal of food. Thus, tissue renewal programs are not committed to maintain cellular equilibrium; stem cells can remodel organs in response to physiological triggers.

Introduction

Organisms live in dynamic environments where external conditions fluctuate at cyclic or irregular intervals. Over its lifetime, a single animal is likely to experience variation in factors such as climate, mating opportunities, and food availability. The challenge for the adult individual is to effectively adjust its organ systems when faced with environmental volatility (Meyers and Bull, 2002). Although post-developmental tissues are often regarded as homeostatically maintaining a constant size, one type of adult organ plasticity is the induction of growth by actual or anticipated functional demand. Familiar examples include enlargement of skeletal muscles with weight loading, expansion of erythrocyte populations at high altitude, and elaboration of mammary glands during pregnancy. Flexible resizing of adult organs can be regarded as an adaptive response to external change (Piersma and Lindström, 1997). However, little is known about the mechanisms that enable adaptive resizing.

Perhaps the best understood model for adaptive resizing is the vertebrate small intestine. Intermittent feeders such as hibernating squirrels and ambush-hunting snakes exhibit extreme mucosal elaboration and atrophy during cycles of feasting and fasting (Carey, 1990; Secor and Diamond, 1998). Frequent feeders such as laboratory rodents exhibit similar, albeit less dramatic, mucosal changes (Dunel-Erb et al., 2001). The human small intestine can also undergo adaptation, and exhaustion of its adaptive ability leads to disorders such as short bowel syndrome (Drozdowski and Thomson, 2006). During intestinal adaptation,

changes occur in the height and density of crypts and villi, rate of cell turnover, and mitotic index (Brown et al., 1963; Dunel-Erb et al., 2001), suggesting, as in other instances of adaptive organ growth (Ambrosio et al., 2009; Koury, 2005; Visvader, 2009), that progenitor cell populations have been altered. Such data contrast with the view that organ renewal programs uphold tissue homeostasis and maintain constant cell numbers by coordinating the proliferation of stem cells with the loss of differentiated cells. Nonetheless, the molecular and cellular mechanisms of adaptive growth remain poorly understood.

The relative simplicity and tractability of the adult Drosophila midgut (Figure 1A) make it an appealing model to investigate tissue dynamics. The posterior half of the midgut is structurally and functionally similar to the vertebrate small intestine (Miller, 1950). In both cases, multipotent stem cells maintain a simple epithelium containing absorptive enterocytes and secretory enteroendocrine cells, although the fly midgut lacks the small intestine's crypt-villus structure (Losick et al., 2011). Intestinal stem cells in both flies and mammals homeostatically maintain organ size by generating progeny to replace cells lost through regular turnover or acute injury, although the fly has no transit amplifying population (Jiang et al., 2009; Micchelli and Perrimon, 2006; Ohlstein and Spradling, 2006). Fly and mammalian intestinal stem cells also share key regulatory signals such as Notch, Wnt, Epidermal Growth Factor and Hippo (Losick et al., 2011).

Here we demonstrate that stem cells in the adult fly midgut execute a reversible mechanism for organ growth in response to environmental factors. A niche signal helps trigger a shift in collective stem cell behaviors to produce an increase in overall organ cell number. Thus, stem cells act as agents of tissue remodeling, flexibly altering their behavior as guided by physiological cues.

Results

Feeding Activates Concomitant Expansion of Total and Progenitor Cell Populations

After emerging from pupal metamorphosis, newly-eclosed Drosophila adults represent a ‘naïve’ digestive state without ingested nutrients. To investigate the midgut response to food, we began by assessing when feeding commences. Monitoring of individual animals showed that adult females start to feed between 2 and 19 hours, with a median time of 5 hours (Figure 1B). These data guided selection of three ages for further study: 0-2 hour adults (hereafter called 0 day), considered ‘food-naïve’; 1-day adults, which have recently started feeding; and 4-day adults, which have full gastrointestinal mobilization. Midguts at these times exhibited similar anatomical shapes but substantial differences in gross size. Compared to day 0, guts appeared progressively larger after 1 and 4 days of feeding but not fasting (Figure 1C). The sizes of two other known nutrient-sensitive tissues, the fat body and ovary (Drummond-Barbosa and Spradling, 2001), were also altered by feeding; however, sizes of most other organs and overall body length remained comparable.

Organ enlargement could result from addition of new cells, increases in cell size, or physical distention. To investigate the possibility of additional cells without confounding factors such as region- and diet-specific variation in cell size and density, we developed a ‘census’ protocol to comprehensively count all cells in a subregion of interest on a single-gut basis (Supplemental Figure S1). We focused on the distal midgut loop bound by two stereotypic constrictions in the gut tube, which may demarcate digestive compartments (Figure 1A, right). This ‘distal hairpin’ has a high abundance of midgut progenitors, suggestive of dynamic tissue behavior.

In the distal hairpin, total number of midgut cells increased by ~300% over 4 days of feeding (Figure 1H and Supplemental Table S1). Some of this increase occurred between

days 0 and 1 irrespective of diet, but most occurred between days 1 and 4 specifically in fed animals. At day 4, cell number in fed guts exceeded fasted cohorts by ~220% (Figure 1H and Supplemental Table S1). This increase in total cells shows that the midgut grows in response to feeding.

What is the source of these additional cells? The midgut lineage has just two progenitor cell types: stem cells and their immature daughters, called enteroblasts (Figure 1D) (Ohlstein and Spradling, 2006). Stem cells are the only mitotic cells in the tissue; enteroblasts terminally differentiate without further divisions (Ohlstein and Spradling, 2006). Both progenitors are diploid cells marked by *escargot* (Micchelli and Perrimon, 2006; Ohlstein and Spradling, 2007); enteroblasts also express the Notch activity reporter *Suppressor of Hairless* (*Su(H)lacZ*) (Ohlstein and Spradling, 2007). Within the epithelium, stem cells reside in a basal niche formed, at least in part, by visceral muscle (Biteau and Jasper, 2011; Buchon et al., 2010; Jiang and Edgar, 2009; Lin et al., 2008). Enteroblasts localize apically to their mother stem cell (Micchelli and Perrimon, 2006; Ohlstein and Spradling, 2007). Ninety percent of enteroblasts differentiate into polyploid enterocytes that form the intestinal epithelium, while 10% differentiate into enteroendocrine cells (Ohlstein and Spradling, 2006).

Since enteroblasts are transient intermediates, their dynamics are indicative of recent stem cell activity. We thus examined the effect of feeding on enteroblast number. Enteroblasts were nearly absent from 0-day guts but appeared in limited numbers in 1-day fed and fasted guts (Figures 1E and 1I and Supplemental Table S1). After 4 days, enteroblasts became highly abundant in fed guts, outnumbering fasted cohorts by ~230% (Figures 1F, 1G, and 1I and Supplemental Table S1). The marked increase in enteroblasts between days 1 and 4 suggests that feeding stimulates production of new stem cell progeny. Interestingly, feeding also caused expansion of the stem cell population itself. In 4-day fed guts, stem cells were ~240% more numerous than in 0-day guts and ~160% more numerous than in 4-day fasted guts (Figures 1F, 1G, and 1J, and Supplemental Table S1). Altogether, the coordinated dynamics of total, enteroblast, and stem cell populations are consistent with a model in which feeding elicits midgut growth through stem cell activation.

Increased Stem Cell Divisions Account for Feeding-Induced Growth

To explicitly investigate the effects of feeding on stem cell divisions, we compared the evolution of stem cell clones in fed and fasted guts. Single, labeled stem cells were generated in 0-day guts through induced expression of a heritable *tub-lacZnls* transgene (Harrison and Perrimon, 1993) (Figure 2A). The 0-day animals were divided into fed and fasted cohorts, and the evolution of clones originating from the marked, 0-day stem cells was compared between the two cohorts at various times. Importantly, all marked progeny in the distal hairpin of each midgut were quantified to determine the behavior of the stem cell population in aggregate.

Since enteroblasts remain adjacent to their mother stem cell, the number of contiguous cells in a clone reveals the number of asymmetric daughter fates (Micchelli and Perrimon, 2006; Ohlstein and Spradling, 2006). In the distal hairpin of 0-day guts, 90% of clones were single diploid cells, presumably stem cells (Figures 2A and 2D, and Supplemental Table S2). In 1-day fed and fasted guts, the proportion of multicell clones—mostly pairs of diploid cells—rose to ~40% (Figure 2D and Supplemental Table S2). In 4-day fed guts, clones containing ≥3 cells became more common and often included polyploid enterocytes, whereas 4-day fasted guts appeared similar to 1-day (Figures 2B-D and Supplemental Table S2). Thus after day 1, feeding accelerates stem cell production of differentiated daughters.

These findings indicate that asymmetric divisions contribute to growth. However, the production of differentiated daughters was insufficient to account for the ~300% expansion of total cells documented by the census (Figure 1H). The presence of more stem cells in fed guts (Figure 1J) raised the possibility that symmetric divisions might also contribute to growth. Suggestively, we observed occasional 2-cell clones with a basal-basal arrangement —placing both daughters in proximity to the visceral muscle niche—instead of the basal-apical relationship associated with stem cell-enteroblast pairs (Figure 2E) (Ohlstein and Spradling, 2007).

If new stem cells are created by symmetric divisions and then disperse, an increased number of individual clones would be observed in each gut over time. To test this possibility, we counted all distinct, contiguous clones in the distal hairpins of fed and fasted guts (Figure 2F and Supplemental Table S2). Compared to 0-day guts, the number of individual clones per gut increased ~400% in 1-day fed and fasted guts. The number of clones continued to rise in 4-day fed guts, becoming ~900% greater than at day 0; no further increase occurred in 4-day fasted guts. This result indicates that midgut stem cells can generate new lineages through symmetric divisions and further suggests that feeding increases the frequency of these divisions.

Strikingly, the integrated contributions of asymmetric and symmetric divisions can quantitatively account for the net increase in total cells of 4-day fed guts (Supplemental Table S3). Based on census data of stem cells and total cells (Figures 1H and 1J), each stem cell in the midgut at day 0 would need to give rise to an average of 15 new cells to collectively produce a 300% increase in total cells at 4 days. In this population-level clone analysis, each marked 0-day stem cell gave rise to an average of 17 new cells at 4 days (see Supplemental Table S3). These calculations strongly implicate excess stem cell divisions as the direct source of feeding-induced growth.

Inverse Ratios of Symmetric and Asymmetric Divisions During Growth

The evolution of *lacZ*-marked clone populations argues that symmetric divisions contribute to midgut growth. However, the *lacZ* system cannot distinguish the lineages of two sister stem cells since both are labeled with the same marker. To directly visualize symmetric and asymmetric lineages, we turned to twin-spot Mosaic Analysis with Repressible Cell Markers (MARCM) (Yu et al., 2009). In this technique, heat shock-induced mitotic recombination differentially labels the two daughters of a stem cell division with heritable expression of either GFP or RFP (Figure 3A). The individual fates of marked daughter pairs can then be assessed through the resultant twin spots, which exhibit distinct signatures for asymmetric and symmetric fate outcomes based on the subsequent behaviors of each daughter cell (Figure 3B; see also Supplemental Experimental Procedures).

Consistent with *lacZ* clone data, midgut twin spots revealed both symmetric and asymmetric lineages. In symmetric twin spots, both separated and contiguous lineages were observed (Figure 3D). The existence of separated, multicell twin spots (Figure 3D left) is consistent with the rise in numbers of *lacZ* clones over time (Figure 2F). Together, these data support the view that at least some sister stem cells do not remain juxtaposed within the epithelium. Contiguous twin spots (Figure 3D right) generally contained more cells than separated twin spots; the two branches of a contiguous lineage could exhibit similar or dissimilar proliferation rates and intermingle in a variety of patterns.

In asymmetric twin spots (Figure 3C), first-born enterocytes (arrows) remained in contact with their mother stem cell lineage. No lone detached enterocytes were observed, confirming that enteroblast daughters do not scatter from their mother stem cell (Micchelli and Perrimon, 2006; Ohlstein and Spradling, 2006). Regularly, one-color cell clusters

appeared in proximity to asymmetric twin spots (cross, Figure 3C right). Each cluster invariably contained at least one diploid cell, and the cluster label matched the stem cell lineage of the nearby twin spot. This pattern suggests that one-color clusters arose through creation and dispersal of new stem cells from the stem cell lineage of asymmetric twin spots. Thus, at least some individual stem cells appear to switch between asymmetric and symmetric modes.

Twin-spot MARCM provides a retrospective ‘snapshot’ of symmetric and asymmetric division frequencies at the time of induction. We took advantage of this feature to compare divisions in the distal hairpin under fed and fasted conditions (Figure 3E; see Experimental Procedures for details). When induced in 2-day fed guts, which are undergoing expansion of total and stem cell populations, 68% of the resultant twin spots had symmetric signatures and 32% had asymmetric signatures. In 2-day fasted guts, although low overall proliferation stalled many twin spots, proportions were inverted to 31% symmetric and 69% asymmetric. Induction of twin spots in 7-day fed guts, which are considered to be at homeostasis (Buchon et al., 2010; Jiang et al., 2009), produced a ratio of 41% symmetric to 59% asymmetric. Thus, inverse proportions of symmetric and asymmetric divisions were not simply due to the presence or absence of food. Rather, predominant symmetric divisions may be a hallmark of non-homeostatic growth.

Acute Upregulation of Local but not Systemic Insulin Correlates with Organ Growth

We next sought to determine the signals that link feeding to proliferation and growth. The most attractive candidate was the insulin pathway, whose central roles in nutrient sensing and growth control are broadly conserved. In flies, most of insulin's systemic roles are mediated by a cluster of specialized brain neurons that secrete dILPs 2, 3, and 5 into humoral circulation (Figure 4A) (Broughton et al., 2005; Ikeya et al., 2002).

To assess the relationship between feeding and systemic insulin, we examined expression kinetics of the three major *dilps*. As expected, *dilp2* and *dilp5* (although not *dilp3*) were upregulated in the brains of 4-day fed animals compared to 0-day and 4-day fasted animals as indicated by reporter expression and qPCR (Figures 4D and 4F). However, in 1-day fed animals *dilp2* was not increased, while *dilp5* exhibited modest upregulation (Figures 4D and 4F). Since feeding commences before day 1 (Figure 1B), these kinetics suggest that systemic insulin is not acutely sensitive to food intake.

We considered whether a more proximal cue might signal the arrival of food in the gut. Veenstra *et al.* (2008) reported expression of a single insulin peptide, dILP3, in midgut visceral muscle. Strikingly, midgut dILP3 is restricted to a subregion of circular fibers that largely coincides with the progenitor-enriched distal hairpin (Figure 4B). Visceral muscle, considered to be part of the niche, is a source of numerous stem cell regulatory factors (Biteau and Jasper, 2011; Jiang and Edgar, 2011; Buchon et al., 2010; Jiang and Edgar, 2009; Lin et al., 2008). Indeed, basally-localized stem cells closely appose the dILP3-expressing fibers (Figure 4C).

We evaluated the relationship between feeding and midgut dILP3 (Figures 4E and 4F). At day 0, midgut *dilp3* expression was extremely low as indicated by a *dilp3>lacZ* reporter and qPCR. By day 1, *dilp3* had markedly increased in both fed and fasted guts, surpassing systemic upregulation and correlating with the early, food-independent increase in total and progenitor cells (Figures 1H-J). Between days 1 and 4, *dilp3* continued to rise dramatically in fed but not fasted guts, correlating with the later, food-dependent increase in cell numbers. Thus, the kinetics of local dILP3 coincide with the dynamics of stem cell proliferation and organ growth.

Local Insulin Production is Required for Feeding-Induced Stem Cell Proliferation and Organ Growth

Given the correlation between niche insulin and growth, we sought to determine the functional relevance of midgut dILP3. RNAi-mediated knockdown of *dilp3* in the visceral muscle of adult midguts was performed using the *mef2* driver in conjunction with the TARGET system (*mef2^{ts}>dilp3IR*) (McGuire et al., 2003). We then censused total and progenitor cells in 4-day fed distal hairpins. Remarkably, local depletion of *dilp3* strongly reduced total cell number to ~45% fewer than controls (Figure 5C and Supplemental Table S5). This result demonstrates the necessity of niche insulin for the full growth response. Enteroblast number was reduced by ~35%, and stem cell number showed a similar trend, although the peripheral HRP stain (Figure 4C) used in place of cytoplasmic *esg>GFP* was less robust in the census protocol (Figures 5A and 5C, and Supplemental Table S5). These data establish local dILP3 as a critical regulator of feeding-induced growth.

We also examined whether *mef2*-driven overexpression of dILP3 could bypass the feeding requirement for growth. Again, the TARGET system was used (*mef2^{ts}>dilp3*), and total and progenitor cells were censused in 4-day fasted distal hairpins. dILP3 overexpression increased total cell number to ~100% above controls (Figure 5D and Supplemental Table S5). Moreover, forced dILP3 expression increased enteroblast number by 350%, and stem cell number showed a similar trend (Figures 5B and 5D, and Supplemental Table S5). The cognate effects of *dilp3* manipulations on progenitor and total cell populations suggest a model in which visceral muscle dILP3 promotes stem cell proliferation to drive organ growth upon feeding.

Insulin Receptor Activation in Stem Cells Mediates Feeding-Induced Proliferation

If insulin peptides target stem cells during feeding-induced growth, then insulin receptor activation should occur in the stem cells of fed but not fasted guts. Examination of *tGPH*, a fusion of GFP to a pleckstrin homology (PH) domain (Britton et al., 2002) confirmed this: tGPH was enriched at the stem cell cortex in fed guts (Figure 5E top) but distributed throughout the cytosol in fasted guts (Figure 5E bottom). These contrasting localizations show that feeding activates the endogenous stem cell insulin pathway.

We next investigated whether stem cell-intrinsic insulin signaling is epistatic to feeding-induced proliferation. A single Drosophila Insulin Receptor (dInR) transduces signals from the dILPs (Ikeya et al., 2002) and permits homeostatic stem cell proliferation (Amcheslavsky et al., 2009; Biteau et al., 2010). To test whether loss of dInR makes stem cells refractory to ingested food, we generated clones from *dinr^{339}* null stem cells. Over 4 days of feeding, most *dinr^{339}* stem cells did not proliferate but were stalled as 1-cell clones (Figures 5F and 5H, and Supplemental Table S6). This outcome resembles control stem cell clones in fasted guts and contrasts with the multicell clones arising from control stem cells in fed guts. Thus, dInR is required for feeding-induced stem cell proliferation. To test whether constitutive dInR signaling makes stem cells proliferate without food, we generated stem cells expressing activated dInR (dInR^{ACT}). In both fed and fasted guts, *dinr^{ACT}* stem cells produced large clones that often protruded into the lumen (Figure 5G). In fact, clone sizes of fasted guts were highly similar to fed guts (Figures 5I and 5I', and Supplemental Table S6). Thus, dInR^{ACT} bypasses the feeding requirement for stem cell proliferation. Altogether, these findings demonstrate that insulin peptides act directly on stem cells to stimulate proliferation during feeding-induced growth.

Reversal and Recurrence of Growth during a Cycle of Fasting and Refeeding

The data above establish that the onset of feeding invokes a stem cell-driven growth response in the new adult midgut. Is this response a unique and irreversible feature of early

adult life? Alternately, are older adults able to modulate midgut size in response to dietary fluctuation? To distinguish these possibilities, we investigated core parameters of the initial growth response during subsequent phases of fasting and refeeding.

New adults were subjected to an 18-day cycle of 4 days feeding, 7 days fasting, and 7 days refeeding; guts were examined at 4 and 11 day transition points and at 18 days. During this cycle, midguts retained their anatomic shape but shrunk during fasting and enlarged during refeeding (Figure 6A). Distal hairpin censuses revealed that cell number decreased by ~30% when 4-day fed guts were subjected to 7 subsequent days of fasting (fed-fasted guts; Figure 6C and Supplemental Table S7). This decline was accompanied by widespread apoptosis and cell extrusion (Figures 6F and 6G), features not seen with continuous feeding or fasting. After 7 days of refeeding, cell number rebounded in 18-day fed-fasted-refed guts to eventually surpass 4-day fed guts. Whether this surplus reflects a higher size set point or the onset of aging-associated dysplasia (Biteau et al., 2008; Biteau et al., 2010) is not clear. Nonetheless, these findings show that older midguts retain a latent growth response that is reversible and repeatable with dietary change.

To investigate whether stem cell activity underlies the remodeling of older guts, we censused progenitors during the 18-day feed-fast-refeed cycle (Figures 6B and 6D, and Supplemental Table S7). Enteroblast number fluctuated in tandem with total cell number; in particular, a ~60% decline during fasting suggests that diminished stem cell proliferation combines with apoptosis to reduce total cells. Recovery of enteroblast number with refeeding (Figure 6D) (McLeod et al., 2010) indicates the involvement of at least asymmetric stem cell divisions in food-sensitive resizing. Stem cell number differences were not measured as statistically significant, although high variance was apparent in older guts. *dilp3>lacZ* reporter expression decreased during fasting and increased with refeeding (Figure 6E), consistent with involvement of local insulin in stem cell regulation. Thus, core elements of the initial feeding response—upregulation of midgut *dilp3*, generation of surplus progeny, and induction of non-homeostatic growth—recur when food is reintroduced. Qualitatively similar results were obtained when 4-day, continually fasted adults were given food (data not shown). Thus, in later adult life, core parameters of the initial growth mechanism are modulated to resize the midgut in response to dietary change.

Discussion

Flexible Modulation of Tissue Homeostasis

A common view of renewal programs is that they uphold a homeostatic tissue state: stem cells divide to replace lost cells, keeping overall cell number constant (Pellettieri and Alvarado, 2007; Simons and Clevers, 2011). Our data show how an adult tissue exploits its renewal program to adapt to environmental change (Figure 7A). In the fly midgut, cell number is not a fixed attribute but instead oscillates in response to a specific external cue, dietary load. The ability of midgut cell number to fluctuate indicates that in this tissue, homeostasis is best considered as metastable (Figure 7B). We speculate that the organ can, when prompted by cues, switch between different size ‘set points’ in accordance with food abundance. This adaptive resizing may help tune digestive capacity to functional demand, optimizing physiological fitness. How the size set point for each dietary state is established, whether tissues retain a memory of prior states, and whether the sensitivity and flexibility of adaptive transitions degrade over time are issues that arise from this notion of metastable homeostasis.

While adaptive growth is characterized by a homeostasis-breaking increase in total and progenitor cells, we note hints of one parameter that appears homeostatically controlled: the relative *proportion* of stem cells. In the initial growth response and several experimental

manipulations, stem cells (but not enteroblasts) scale isometrically with total cells to remain 15-20% of the total population. This 'stem cell proportionality' suggests that the organ may have a mechanism that actively maintains a constant percentage of stem cells despite variable numbers of total cells.

Local Insulin Regulation during Intestinal Growth

In the midgut, as in other Drosophila stem cell tissues, insulin signaling promotes proliferation during development and homeostasis (Amcheslavsky et al., 2009; Biteau et al., 2010; Britton et al., 2002; Chell and Brand, 2010; Hsu et al., 2008; LaFever and Drummond-Barbosa, 2005; McLeod et al., 2010; Siegrist et al., 2010; Sousa-Nunes et al., 2011) as well as during adaptive growth (this work). The common sensitivity of intestinal, neural, and gonadal stem cells to insulin likely reflects the need to coordinate organ systems and integrate metabolic status with systemic control of growth, longevity, and fecundity.

Our data show that a spatially discrete source of insulin is central to adaptive midgut growth. This source is the visceral muscle niche itself, which upregulates *dilp3* with immediate and sensitive kinetics in response to ingested food and signals directly to adjacent stem cells. The tissue intrinsic nature of the dILP3 pathway linking feeding to growth is akin to local insulin activation of quiescent Drosophila larval neuroblasts (Chell and Brand, 2010; Sousa-Nunes et al., 2011). Crucially, we find that *dilp3* depletion in gut visceral muscle significantly reduces progenitor and total cell numbers, demonstrating a direct functional role for niche signaling. Midgut *dilp3* oscillates dynamically during feeding and fasting in tandem with organ size. In this respect, the fly gut is reminiscent of the mouse small intestine, in which Insulin-like Growth Factor-I (IGF-I) is expressed in subepithelial myofibroblasts and smooth muscle (Pucilowska et al., 2000) and increases during adaptation (Winesett et al., 1995).

Since the intestine controls nutrient delivery to the rest of the body, rapid production of insulin in the midgut may be a critical mechanism to 'jumpstart' growth at the site of food absorption, potentiating nutrient delivery to more distal tissues. Circulating dILPs appear to complement local dILP3 since midgut *dilp3* depletion does not completely replicate fasting or stem cell-intrinsic loss of dInR. We suggest that midgut dILP3, responding to proximate ingestion of food, and systemic dILPs, reflecting organism-wide metabolic status, are integrated at the level of the stem cell. These discrete insulin sources may cooperate to tune the growth response in keeping with the midgut's dual status as both the entry point for nutrients and as a component of multi-organ physiological axes.

Stem cell dynamics during organ adaptation

In the midgut, the stem cell is central to adaptive growth: it both receives the insulin signal and executes the proliferative response. Our study identifies two key features of adaptive stem cell dynamics: divisions in excess of homeostatic maintenance and altered proportions of symmetric and asymmetric fate outcomes.

As in many mammalian organs, stem cells in the fly midgut have previously been shown to maintain cellular homeostasis in the face of injury and infection (Buchon et al., 2010; Buchon et al., 2009; Jiang et al., 2009). Conversely, loss of homeostatic stem cell proliferation is a hallmark of tumor initiation and aging (Apidianakis et al., 2009; Biteau et al., 2008; Lee et al., 2009; Rossi et al., 2008). Adaptive growth stands in contrast to both modalities. Here, stem cells break homeostasis and generate surplus cells without loss of tissue integrity. This 'excess' proliferation occurs in the context of normal physiology, and far from being pathological, it may serve to optimize organ function. Understanding the

mechanisms that enable deviations from homeostasis in healthy organs may help inform detrimental loss of homeostasis in disease.

Whereas stem cell divisions during non-growth states tend to generate differentiated cells, divisions during adaptive growth tend to generate new stem cells. One possible rationale for this switch is to distribute the burden of maintaining a larger organ among more individual stem cells, likely a relevant factor in a lineage without transit amplifying divisions. Another, non-exclusive rationale comes from mathematical models suggesting that feedback modulation of symmetric divisions is fundamental to tissue robustness during growth, repair, and maintenance (Lander et al., 2009). Indeed, our data indicate that even during non-growth periods, symmetric fates occur approximately once out of every three stem cell divisions. The regular occurrence of fate symmetry, and the ability of at least some stem cells to switch between symmetric and asymmetric modes, raise the possibility that stochastic competition creates a pattern of neutral drift akin to the mouse small intestine (Simons and Clevers, 2011). Whether fate regulation is intrinsic or extrinsic to the dividing stem cell, and how symmetric:asymmetric ratios are modulated during homeostasis and growth are key questions that emerge from our findings.

In general, the same qualities that make stem cells the linchpin of tissue renewal programs—their ability to produce differentiated progeny and to self-renew—also make them ideal agents of adult tissue adaptation. Collective alterations in stem cell behaviors provide a flexible mechanism for organ size control and reveal unanticipated plasticity within the stem cell population itself. Does population-level plasticity originate in hardwired differences between individual stem cells? Alternately, does it arise through biasing the probabilities of stochastic behaviors across a population of equivalent stem cells? The adaptive growth response of the adult Drosophila midgut provides a platform to investigate these material issues.

Experimental Procedures

Fly Stocks and Feeding Regimens

For stocks, husbandry, and first meal assay, see Supplemental Experimental Procedures. For feeding and fasting regimens, females were collected 0-2 hours post-eclosion. Fed animals were given yeast paste (1 g/1.4 ml H_2O) plus cornmeal/molasses food. Fasted animals were given water only, except during the fasted phase of feed-fast-refeed experiments where animals were given 1% w:v sucrose in water.

Immunohistochemistry and Microscopy

Midguts and brains were fixed *in situ* 20 min. at room temperature in 8% formaldehyde, 200 mM Na cacodylate, 100 mM sucrose, 40mM KOAc, 10mM NaOAc, and 10mM EGTA. Tissues were immunostained (see Supplemental Experimental Procedures for antibodies) and mounted in agarose for brightfield and confocal microscopic analysis.

Distal Hairpin Identification and Cell Censuses

The distal hairpin was identified as the region bounded by the first constriction in the muscle sheath distal to the copper cells and the first prominent kink in the gut tube distal to its posterior 180° turn (Figure 1A). Cell number in this region was comprehensively determined through a census protocol based on Cell Profiler analysis (Carpenter et al., 2006) of confocal reconstructions (see Supplemental Experimental Procedures and Supplemental Figure S1). Statistical tests were performed using StatPlus:Mac software.

Clone Induction and Analysis

LacZ and MARCM stem cell clones were induced 52-57 h after puparium formation by a single 90 minute heat shock at 38.5 °C to activate FLP recombination in dividing cells. Twin spots were induced in adults at the indicated ages by a single 60 minute heat shock at 37 °C. See Supplemental Experimental Procedures for details of clone quantitation and twin spot scoring.

RT-qPCR

mRNA was extracted from midguts or brains (5 animals/experiment) followed by cDNA synthesis with Invitrogen SuperStrand III First Script Super Mix (Invitrogen). Real-time PCR was performed using the standard curve method with SYBR GreenER Supermix (Invitrogen) on a StepOnePlus ABI machine. Brain expression levels were normalized to *Su(var)205/HP1a*, and midgut expression levels were normalized to *mef2*. Primer sequences are listed in Supplemental Experimental Procedures.

Supplementary Material

Refer to Web version on PubMed Central for supplementary material.

Acknowledgments

We appreciate generous gifts of reagents from the following: B. Ohlstein, B. Edgar, J. Veenstra, H. Stocker, E. Rulifson, L. Jones, T. Lee, the Bloomington Drosophila Stock Center, and TRiP at Harvard Medical School (NIH/NIGMS R01-GM084947) for fly stocks, and S. Stowers and the Developmental Studies Hybridoma Bank for antibodies. We are particularly grateful to B. Ohlstein for technical advice and helpful discussions. We further thank J. Freimer for MATLAB coding; and T. Nystul, S. Siegrist, J. Thaler, K. Siller, L. Skwarek, A. Wurmser, L. Jones, X. Li, J. Schoenfeld, and I. Hariharan for invaluable comments. L.E.O. was a Genentech Foundation Fellow of the Life Sciences Research Foundation and is supported by NIH K01DK083505. This work was supported by NIH R01GM068675 to D.B.

References

Ambrosio F, Kadi F, Lexell J, Fitzgerald GK, Boninger ML, Huard J. The effect of muscle loading on skeletal muscle regenerative potential: an update of current research findings relating to aging and neuromuscular pathology. Am J Phys Med Rehabil. 2009; 88:145–155. [PubMed: 19169178]

Amcheslavsky A, Jiang J, Ip YT. Tissue damage-induced intestinal stem cell division in Drosophila. Cell Stem Cell. 2009; 4:49–61. [PubMed: 19128792]

Apidianakis Y, Pitsouli C, Perrimon N, Rahme L. Synergy between bacterial infection and genetic predisposition in intestinal dysplasia. Proc Natl Acad Sci USA. 2009; 137:3615–3624.

Biteau B, Hochmuth CE, Jasper H. JNK activity in somatic stem cells causes loss of tissue homeostasis in the aging Drosophila gut. Cell Stem Cell. 2008; 3:442–455. [PubMed: 18940735]

Biteau B, Jasper H. EGF signaling regulates the proliferation of intestinal stem cells in Drosophila. Development. 2011; 138:1045–1055. [PubMed: 21307097]

Biteau B, Karpac J, Supoyo S, Degennaro M, Lehmann R, Jasper H. Lifespan extension by preserving proliferative homeostasis in Drosophila. PLoS Genetics. 2010; 6:e1001159. [PubMed: 20976250]

Britton JS, Lockwood WK, Li L, Cohen SM, Edgar BA. Drosophila's insulin/PI3-kinase pathway coordinates cellular metabolism with nutritional conditions. Dev Cell. 2002; 2:239–249. [PubMed: 11832249]

Broughton SJ, Piper MD, Ikeya T, Bass TM, Jacobson J, Driege Y, Martinez P, Hafen E, Withers DJ, Leevers SJ, et al. Longer lifespan, altered metabolism, and stress resistance in Drosophila from ablation of cells making insulinlike ligands. Proc Natl Acad Sci U S A. 2005; 102:3105–3110. [PubMed: 15708981]

Brown HO, Levine ML, Lipkin M. Inhibition of intestinal epithelial cell renewal and migration induced by starvation. Am J Physiol. 1963; 205:868–872. [PubMed: 5877415]

Buchon N, Broderick NA, Kuraishi T, Lemaitre B. Drosophila EGFR pathway coordinates stem cell proliferation and gut remodeling following infection. BMC Biol. 2010; 8:152. [PubMed: 21176204]

Buchon N, Broderick NA, Poidevin M, Pradervand S, Lemaitre B. Drosophila intestinal response to bacterial infection: activation of host defense and stem cell proliferation. Cell Host Microbe. 2009; 5:200–211. [PubMed: 19218090]

Carey HV. Seasonal changes in mucosal structure and function in ground squirrel intestine. Am J Physiol. 1990; 259:R385–392. [PubMed: 2386247]

Carpenter AE, Jones TR, Lamprecht MR, Clarke C, Kang IH, Friman O, Guertin DA, Chang JH, Lindquist RA, Moffat J, et al. CellProfiler: image analysis software for identifying and quantifying cell phenotypes. Genome Biol. 2006; 7:R100. [PubMed: 17076895]

Chell JM, Brand AH. Nutrition-responsive glia control exit of neural stem cells from quiescence. Cell. 2010; 143:1161–1173. [PubMed: 21183078]

Drozdowski L, Thomson AB. Intestinal mucosal adaptation. World J Gastroenterol. 2006; 12:4614–4627. [PubMed: 16937429]

Drummond-Barbosa D, Spradling AC. Stem cells and their progeny respond to nutritional changes during Drosophila oogenesis. Dev Biol. 2001; 231:265–278. [PubMed: 11180967]

Dunel-Erb S, Chevalier C, Laurent P, Bach A, Decrock F, Le Maho Y. Restoration of the jejunal mucosa in rats refed after prolonged fasting. Comp Biochem Physiol A Mol Integr Physiol. 2001; 129:933–947. [PubMed: 11440878]

Harrison DA, Perrimon N. Simple and efficient generation of marked clones in Drosophila. Curr Biol. 1993; 3:424–433. [PubMed: 15335709]

Hsu HJ, LaFever L, Drummond-Barbosa D. Diet controls normal and tumorous germline stem cells via insulin-dependent and -independent mechanisms in Drosophila. Developmental Biology. 2008; 313:700–712. [PubMed: 18068153]

Ikeya T, Galic M, Belawat P, Nairz K, Hafen E. Nutrient-dependent expression of insulin-like peptides from neuroendocrine cells in the CNS contributes to growth regulation in Drosophila. Curr Biol. 2002; 12:1293–1300. [PubMed: 12176357]

Jiang H, Grenley MO, Bravo MJ, Blumhagen RZ, Edgar BA. EGFR/Ras/MAPK signaling mediates adult midgut epithelial homeostasis and regeneration in Drosophila. Cell Stem Cell. 2011; 8:84–95. [PubMed: 21167805]

Jiang H, Patel PH, Kohlmaier A, Grenley MO, McEwen DG, Edgar BA. Cytokine/Jak/Stat signaling mediates regeneration and homeostasis in the Drosophila midgut. Cell. 2009; 137:1343–1355. [PubMed: 19563763]

Koury MJ. Erythropoietin: the story of hypoxia and a finely regulated hematopoietic hormone. Exp Hematol. 2005; 33:1263–1270. [PubMed: 16263408]

LaFever L, Drummond-Barbosa D. Direct control of germline stem cell division and cyst growth by neural insulin in Drosophila. Science. 2005; 309:1071–1073. [PubMed: 16099985]

Lander AD, Gokoffski KK, Wan FYM, Nie Q, Calof AL. Cell lineages and the logic of proliferative control. Plos Biol. 2009; 7:e15. [PubMed: 19166268]

Lee WC, Beebe K, Sudmeier L, Micchelli CA. Adenomatous polyposis coli regulates Drosophila intestinal stem cell proliferation. Development. 2009; 136:2255–2264. [PubMed: 19502486]

Lin G, Xu N, Xi R. Paracrine Wingless signalling controls self-renewal of Drosophila intestinal stem cells. Nature. 2008; 455:1119–1123. [PubMed: 18806781]

Losick V, Morris L, Fox D, Spradling A. Drosophila stem cell niches: a decade of discovery suggests a unified view of stem cell regulation. Developmental Cell. 2011; 21:159–171. [PubMed: 21763616]

McGuire SE, Le PT, Osborn AJ, Matsumoto K, Davis RL. Spatiotemporal rescue of memory dysfunction in Drosophila. Science. 2003; 302:1765–1768. [PubMed: 14657498]

McLeod CJ, Wang L, Wong C, Jones DL. Stem cell dynamics in response to nutrient availability. Curr Biol. 2010; 20:2100–2105. [PubMed: 21055942]

Meyers L, Bull J. Fighting change with change: adaptive variation in an uncertain world. Trends in Ecology & Evolution. 2002; 17:551–557.

Micchelli CA, Perrimon N. Evidence that stem cells reside in the adult Drosophila midgut epithelium. Nature. 2006; 439:475–479. [PubMed: 16340959]

Miller, A. Internal Anatomy of the Imago. In: Demerec, M., editor. Biology of Drosophila. New York: Wiley & Sons; 1950. p. 420-534.

Ohlstein B, Spradling A. The adult Drosophila posterior midgut is maintained by pluripotent stem cells. Nature. 2006; 439:470–474. [PubMed: 16340960]

Ohlstein B, Spradling A. Multipotent Drosophila intestinal stem cells specify daughter cell fates by differential notch signaling. Science. 2007; 315:988–992. [PubMed: 17303754]

Pellettieri J, Alvarado AS. Cell turnover and adult tissue homeostasis: from humans to planarians. Annu Rev Genetics. 2007; 41:83–105. [PubMed: 18076325]

Piersma T, Lindström Å. Rapid reversible changes in organ size as a component of adaptive behaviour. Trends in Ecology & Evolution. 1997; 12:134–138. [PubMed: 21238009]

Pucilowska JB, McNaughton KK, Mohapatra NK, Hoyt EC, Zimmermann EM, Sartor RB, Lund PK. IGF-I and procollagen alpha1(I) are coexpressed in a subset of mesenchymal cells in active Crohn's disease. Am J Physiol Gastrointest Liver Physiol. 2000; 279:G1307–1322. [PubMed: 11093955]

Rossi DJ, Jamieson CHM, Weissman IL. Stem cells and the pathways to aging and cancer. Cell. 2008; 132:681–696. [PubMed: 18295583]

Secor SM, Diamond J. A vertebrate model of extreme physiological regulation. Nature. 1998; 395:659–662. [PubMed: 9790187]

Siegrist SE, Haque NS, Chen CH, Hay BA, Hariharan IK. Inactivation of both foxo and reaper promotes long-term adult neurogenesis in Drosophila. Curr Biol. 2010; 20:643–648. [PubMed: 20346676]

Simons BD, Clevers H. Strategies for homeostatic stem cell self-renewal in adult tissues. Cell. 2011; 145:851–862. [PubMed: 21663791]

Sousa-Nunes R, Yee LL, Gould AP. Fat cells reactivate quiescent neuroblasts via TOR and glial insulin relays in Drosophila. Nature. 2011; 471:508–512. [PubMed: 21346761]

Veenstra JA, Agricola HJ, Sellami A. Regulatory peptides in fruit fly midgut. Cell and Tissue Research. 2008; 334:499–516. [PubMed: 18972134]

Visvader JE. Keeping abreast of the mammary epithelial hierarchy and breast tumorigenesis. Genes & Development. 2009; 23:2563–2577. [PubMed: 19933147]

Winesett DE, Ulshen MH, Hoyt EC, Mohapatra NK, Fuller CR, Lund PK. Regulation and localization of the insulin-like growth factor system in small bowel during altered nutrient status. Am J Physiol. 1995; 268:G631–640. [PubMed: 7537456]

Yu HH, Chen CH, Shi L, Huang Y, Lee T. Twin-spot MARCM to reveal the developmental origin and identity of neurons. Nat Neurosci. 2009; 12:947–953. [PubMed: 19525942]

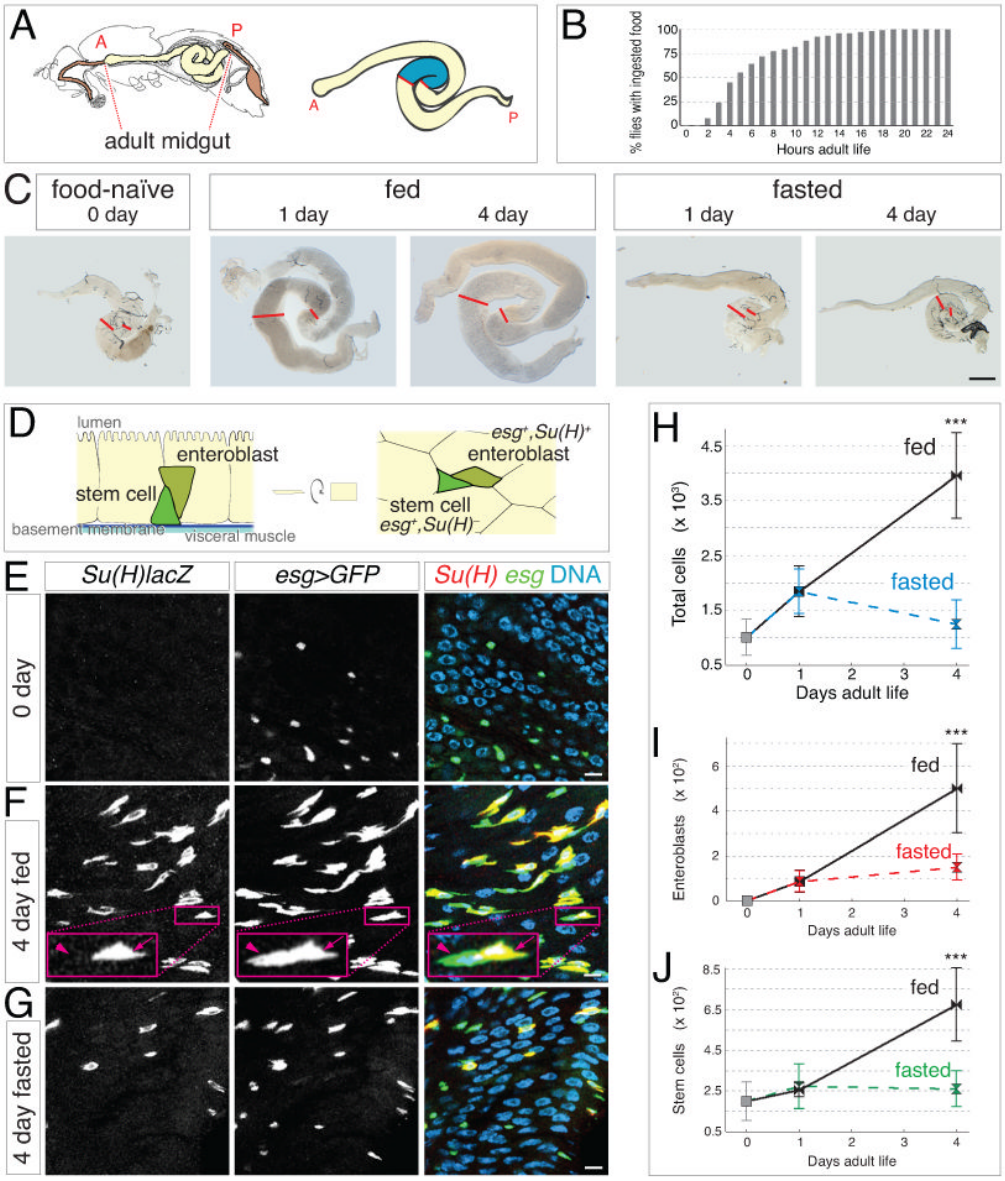

Figure 1. Food intake stimulates concomitant expansion of total and progenitor cell populations in new adult midguts

(A) Left, sagittal view of adult fly gastrointestinal tract (modified from (Miller, 1950)). Right, expanded view of midgut with the distal hairpin region in blue. Anterior (A) and posterior (P) ends of the midgut are indicated.

(B) Commencement of adult food intake. Mean age at first meal is 6.4 ±3.9 hours (S.E.M.), and median age is 5 hours. n = 113.

(C) Gross midgut size increases in fed but not fasted animals during the first 4 days of adult life. Red lines show boundaries of distal hairpin region. Scale bar, 0.5 mm.

(D) Anatomy and markers of midgut progenitors. Stem cells (*esg*$^{+}$, *Su(H)lacZ*$^{-}$) are at the basal surface of the intestinal epithelium, adjacent to basement membrane and visceral muscle layers. Enteroblasts (*esg*$^{+}$, *Su(H)lacZ*$^{+}$) localize apically to their mother stem cell. Characteristic appearance of mother stem cell-daughter enteroblast pairs is shown in cross section (left) and grazing section (right).

(E-G) Feeding increases the abundance of enteroblasts and stem cells. *Su(H)lacZ*, *esg>GFP* midguts were stained for β-galactosidase (red), GFP (green), and DNA (blue). (E) 0-day guts. Enteroblasts (yellow in merge) are nearly absent, suggesting that stem cells (green in merge) are inactive. (F) After 4 days of feeding, enteroblasts (arrow) and stem cells (arrowhead) are more abundant. (G) In 4-day fasted guts, enteroblasts are less abundant and stem cells are sparse. All scale bars, 5 μm.

(H-J) Comprehensive censuses of the distal hairpin. (H) ~300% increase in total cells between 0-day guts and 4-day fed guts but not 4-day fasted guts. (I) Enteroblasts are nearly absent in 0-day guts, increase substantially in 4-day fed guts, and increase to a far lesser extent in 1-day fed and fasted guts and 4-day fasted guts. (J) ~240% increase in stem cells between 0-day guts and 4-day fed guts but not 4-day fasted guts. Data are means ± S.D; $p<0.00005$. See also Supplemental Figure S1 and Supplemental Table S1.

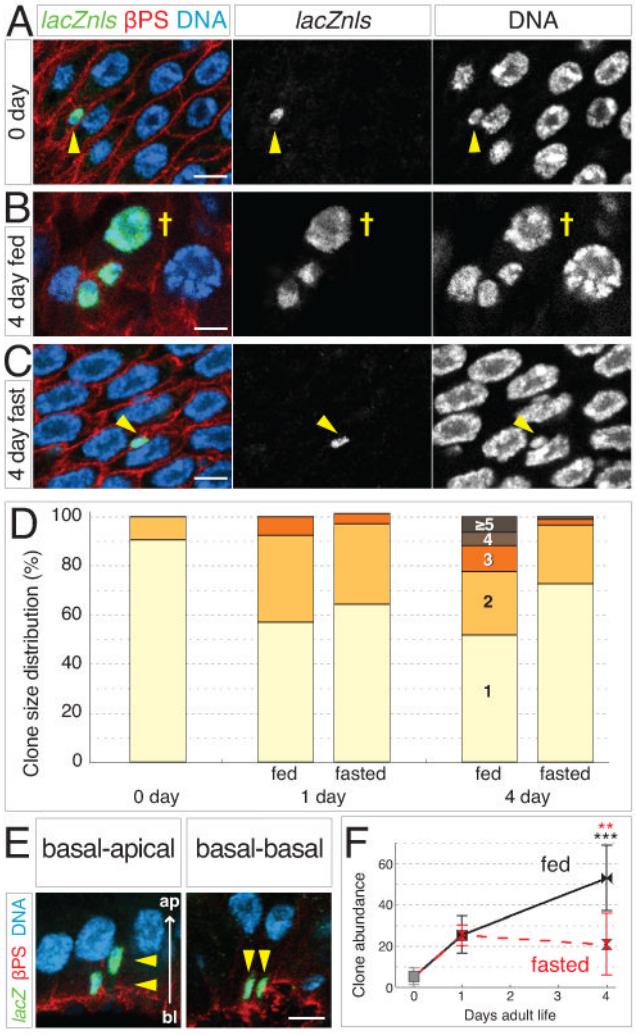

Figure 2. Feeding increases the size and abundance of individual stem cell clones

(A-C) Stem cell clones grow larger in fed guts. Clones labeled with *tub-lacZnls* in green; DNA is blue and βPS integrin outlines cells in red. (A) At 0 days, most labeled cells are single, stem-like cells (arrowhead). (B) In 4-day fed guts, multicell clones are numerous and include polyploid enterocytes (cross). (C) In 4-day fasted guts, most labeled cells remain as single stem-like cells (arrowhead). Scale bars, 5 μm.

(D) Feeding promotes clone growth. At 0 day, nearly all clones contain one cell. In 1-day fed and fasted guts, the proportion of 2-cell clones increases. In 4-day fed guts, clones containing 3 or more cells have become more prevalent. In 4-day fasted guts, 1-cell clones remain predominant. See also Supplemental Table S2.

(E) In cross sections of the gut epithelium, 2-cell clones exhibit either basal-apical (left) or basal-basal arrangements (right). Scale bar, 5 μm.

(F) Feeding increases clone abundance. Between 0 and 1 day, clone abundance (number of discrete clones per distal hairpin) rises 5-fold in fed and fasted guts. In 4-day fed guts, clone abundance has increased to 10-fold higher than at 0 day. In 4-day fasted guts, no further increase occurs. Data are means ± S.D. and obtained from same guts as (D). Black asterisks, p=0.0004 (0 day and 4 day fed); red asterisks, p=0.0026 (4 day fasted and 4 day fed). See also Supplemental Table S2.

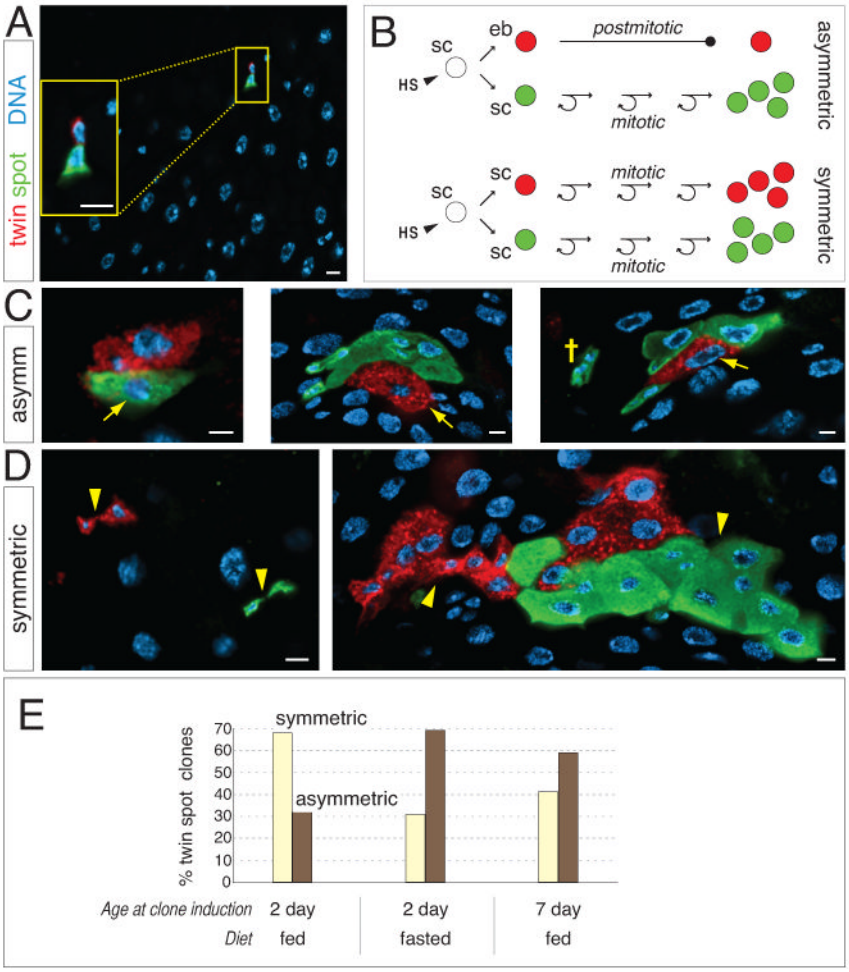

Figure 3. Symmetric stem cell divisions predominate during organ growth

(A) Following clone induction with twin-spot MARCM, the two daughters of a stem cell division are differentially labeled with GFP and RFP (inset). Scale bars, 5 μm.

(B) Schematic cartoon of twin spot fate signatures. HS, heat shock; sc, stem cell; eb, enteroblast.

(C) In asymmetric twin spots, first-born daughter enteroblasts have differentiated into polyploid enterocytes (arrows) and are uniquely labeled. Stem cell daughters have generated additional progeny bearing the alternate label. (Far right) A mono-labeled, 3-cell cluster (cross) near the asymmetric twin spot suggests that a later symmetric division followed the initial asymmetric division. Scale bars, 5 μm.

(D) In symmetric twin spots, both daughters generate additional cells. Sister lineages (arrowheads) can be either separated, implying that stem cells did not remain juxtaposed (left), or contiguous (right). Scale bars, 5 μm.

(E) Quantitation of division modes in fed and fasted guts. Twin spots were induced at the indicated times, and asymmetric and symmetric signatures were scored 4 days later. See also Supplemental Table S4.

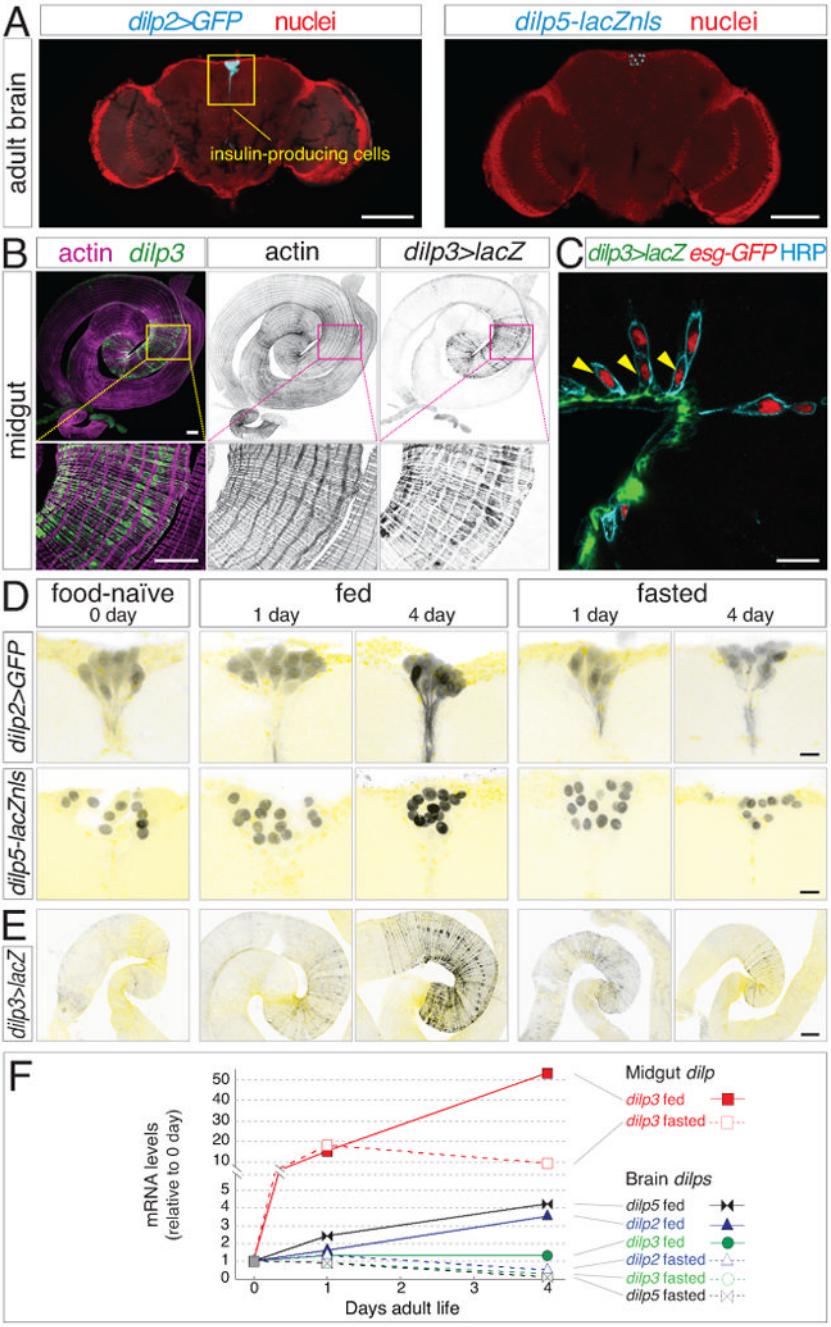

Figure 4. Local insulin production by midgut muscle fibers surpasses systemic insulin upregulation

(A) Expression of *dilp2>GFP* and *dilp5-lacZnls* (cyan) by insulin-producing neurons in the adult brain. Nuclei, red. Scale bars, 100 μm.

(B) Expression of *dilp3* in visceral muscle of the midgut distal hairpin. *dilp3>lacZ* (green, β-galactosidase) colocalizes with actin-rich circular muscle fibers (magenta). Scale bars: 250 μm top, 100 μm bottom.

(C) In cross section, *dilp3*-expressing muscle fibers (*dilp3>lacZ*, green) juxtapose stem cells (arrowheads). Basal stem cells and apical enteroblasts are both marked by nuclear *esg-GFP* (red) and peripheral anti-HRP (cyan). Scale bar, 15 μm.

(D) Brain *dilp2* and *dilp5* reporters are elevated only after 4 days of feeding. Nuclei in pale yellow. Scale bars, 10 μm.
(E) Midgut *dilp3>lacZ* increases after 1 day irrespective of diet and continues to rise with 4 days of feeding but not fasting. Actin in pale yellow. Scale bars, 100 μm.
(F) Local *dilp* upregulation surpasses systemic upregulation. Kinetics of *dilp* mRNA levels in wild type midguts and brains (derived from same animals) as assessed by qPCR. Midgut *dilp3* transcripts increase rapidly with 1 day of feeding (closed red squares) or fasting (open red squares), and continue to rise dramatically with 4 days of feeding but not fasting. Compared to gut *dilp3*, brain *dilps* increase either mildly (*dilp2*, triangles; *dilp5*, bowtie) or not at all (*dilp3*, circles) with feeding; all three decrease below baseline with fasting. One of three representative experiments is shown.

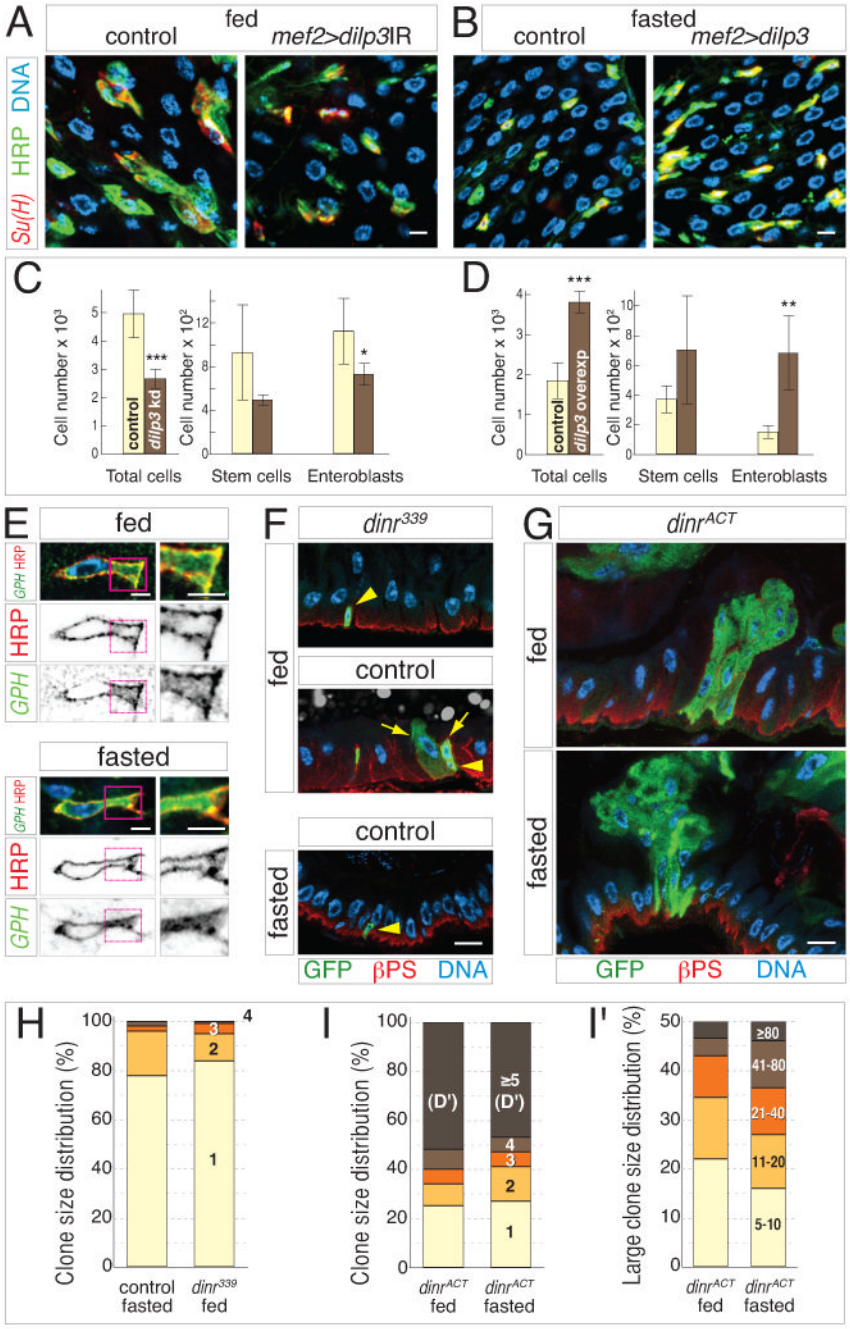

Figure 5. Midgut insulin acts directly on stem cells to induce intestinal growth

(A-B) Midgut dILP3 controls progenitor cell abundance downstream of feeding. Knockdown (*Su(H)lacZ; mef2*^{ts}*>dilp3IR*), overexpression (*Su(H)lacZ; mef2*^{ts}*>dilp3*), and control (*Su(H)lacZ; mef2*^{ts}) midguts were stained for β-galactosidase (red), HRP (green), and DNA (blue). (A) Visceral muscle depletion of *dilp3* reduces the abundance of enteroblasts (HRP^{+}, Su(H)$^{+}$) and stem cells (HRP^{+}, Su(H)) in 4-day fed guts. (B) Exogenous expression of dILP3 in muscle increases the abundance of enteroblasts and stem cells in 4-day fasted guts. Scale bars, 5 μm.

(C-D) Cell censuses of 4-day distal hairpins. (C) In fed guts, visceral muscle knockdown of *dilp3* causes ~2-fold reduction of total cell number and decreased progenitor cell numbers.

(D) In fasted guts, muscle overexpression of *dilp3* causes ~2-fold increase in total cell number and increased progenitor cell numbers. Data are means ± S.D. Total cells, $p<0.0005$; knockdown enteroblasts, $p<0.05$; overexpression enteroblasts, $p<0.01$. See also Supplemental Table S5.

(E) The insulin pathway reporter tGPH (green) is enriched at the stem cell plasma membrane (HRP, red) under fed conditions (top) but is uniformly cytosolic under fasted conditions (bottom). DNA in blue. Right panels show enlarged views of stem cell cytoplasm. Scale bars, 2.5 μm.

(F-I) dInR controls stem cell divisions downstream of feeding. (F) dInR is necessary for feeding-induced stem cell divisions. At 4 days, $dinr^{339}$ clones (green; βPS integrin in red and nuclei in blue) contain only 1 cell in fed (top) and fasted (bottom) guts, while control clones (middle) contain multiple cells. Arrows and arrowheads indicate stem cells and committed daughters, respectively. (G) dInR activation is sufficient for stem cell proliferation in the absence of food. At 4 days, $dinr^{ACT}$ clones (green) are comparably large in fed (top) and fasted (bottom) guts. Scale bar, 10 μm. (H) The size distribution of $dinr^{339}$ clones in fed guts resembles control clones in fasted guts. (I) The size distribution of $dinr^{ACT}$ clones in fasted guts resembles $dinr^{ACT}$ clones in fed guts, even for large clones (≥5 cells; detailed in I'). See also Supplemental Table S6.

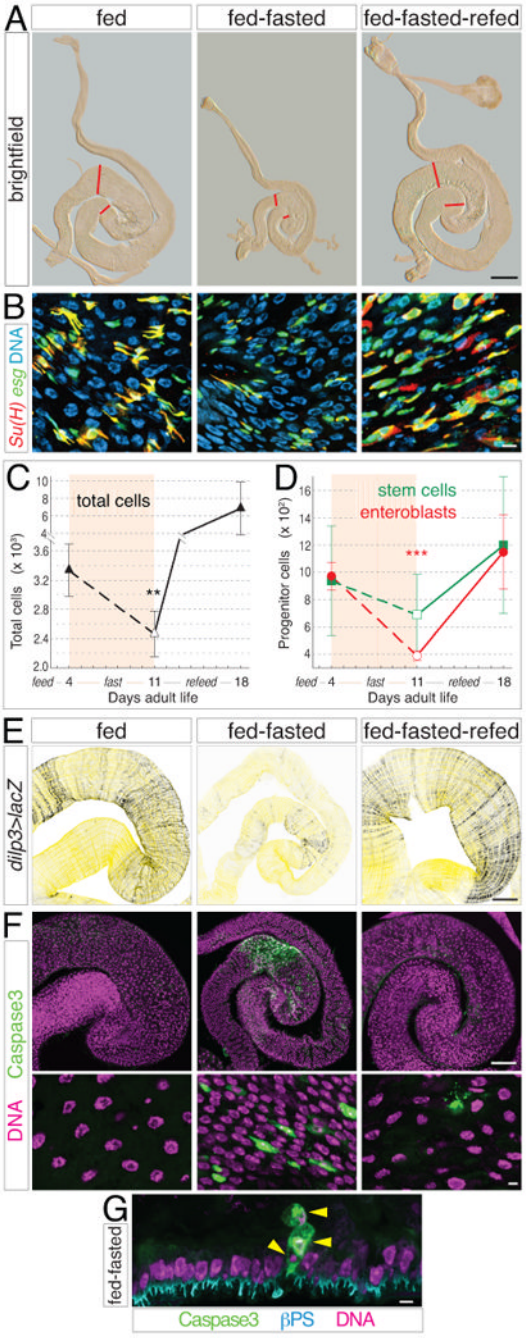

Figure 6. Reversal and recurrence of organ growth during a cycle of fasting and refeeding

(A) Gross size of midguts during a feed-fast-refeed cycle from 0 to 18 days. Midguts from animals raised under the following conditions: 4 days fed, 4 days fed + 7 days fasted, and 4 days fed + 7 days fasted + 7 days refed. Red lines show boundaries of distal hairpin. Scale bar, 0.5 mm.

(B) *Su(H)lacZ, esg>GFP* midguts stained as in Figure 1E. Abundance of enteroblasts is reduced during the fasting phase compared to fed and refed phases. Scale bar, 5 μm.

(C-D) Cell censuses show that total cell number (C) and enteroblast number (D) decrease during fasting and increase during refeeding. Data are means ± S.D. Total cells, $p<0.02$; enteroblasts, $p<0.001$. See also Supplemental Table S7.

(E) *dilp3>lacZ* in midgut visceral muscle is diminished in fed-fasted guts compared to fed and refed guts. Scale bar, 100 μm.
(F) Caspase activation (green, nuclei in magenta) reveals widespread apoptosis in fed-fasted guts but not fed and refed guts. Scale bars, 100 μm (top) and 5 μm (bottom).
(G) Cross section of fed-fasted gut epithelium shows apical extrusion of 3 dying cells (arrowheads) positive for activated caspases (green). βPS integrin (cyan) marks the basal side of the epithelium. Scale bar, 5 μm.

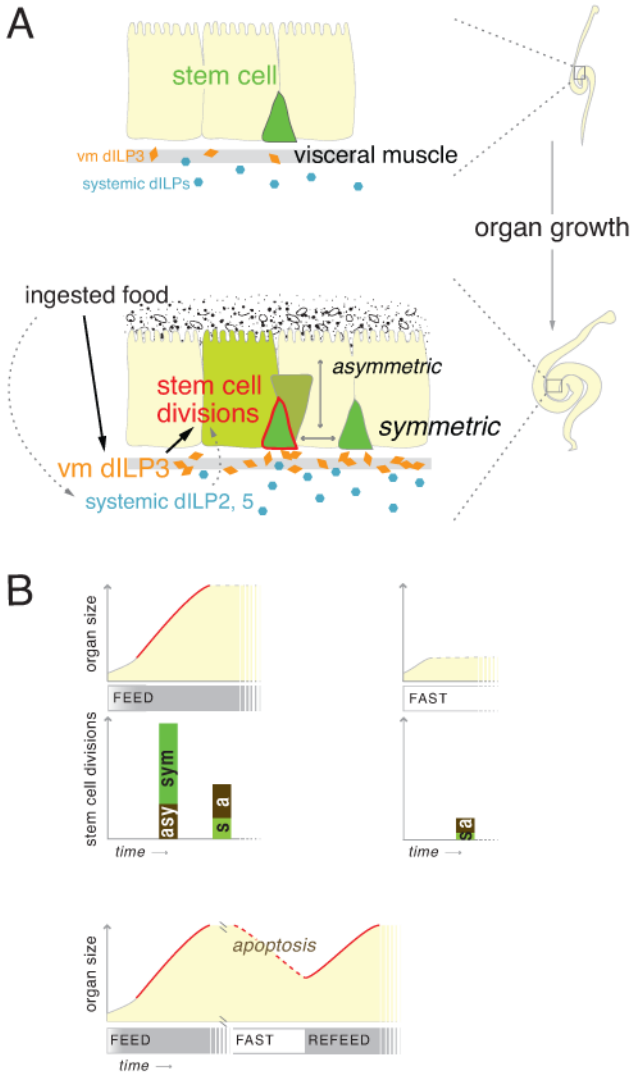

Figure 7. Models

(A) Midgut stem cells direct an adaptive growth response. Without food (top), low dILPs result in stem cell inactivity and smaller organ size. Food ingestion (bottom) acutely upregulates midgut dILP3 and also elevates systemic dILPs. High dILPs activate stem cells to proliferate in excess of maintenance rates. Symmetric and asymmetric divisions combine to increase total cells, producing organ growth.

(B) Externally-induced shifts in stem cell behavior underlie organ size metastability. Over time (x-axes), midguts acquire different numbers of cells (y-axes) based on food availability. Feeding-induced growth (solid red line) arises through increased stem cell divisions (bar height), which are predominantly symmetric (*s*, green bars). Non-growth states (dotted gray lines) have fewer divisions, which are predominantly asymmetric (*a*, brown bars). High apoptosis characterizes degrowth states (dotted red line). Irrespective of diet, a small increase in cell number occurs in new guts (solid gray line).